Available online at www.sciencedirect.com

SciVerse ScienceDirect

Procedia Engineering 39 (2012) 51 – 62

Procedia Engineering

www.elsevier.com/locate/procedia

XIIIth International Scientific and Engineering Conference "HERVICON-2011"

Mechanical Seals With Sliding Surface Texture – Model Fluid Flow and Some Aspects of the Laser Forming of the Texture

Antoszewski Bogdan[a], a[*]

[a]*Kielce University of Technology, Aleja Tysiąclecia Państwa Polskiego 7, PL- 25314 Kielce, Poland*

Abstract

Energy losses resulting from friction between contact surfaces in an internal combustion engine have been studied intensively by a considerable number of tribologists. Still, the automotive industry needs further improvements to reduce friction-related energy losses in engines and drive systems. This problem can be solved by applying porous surfaces generated, for example, by laser surface texturing.

Keywords: Mechanical seals; fluid flow; laser surface texturing; sliding surface.

Energy losses resulting from friction between contact surfaces in an internal combustion engine have been studied intensively by a considerable number of tribologists. Progress in this field has brought numerous economically effective solutions, which enable mass production of motor vehicles. Still, the automotive industry needs further improvements to reduce friction-related energy losses in engines and drive systems. For instance, the losses of energy generated in a piston-ring-cylinder system account for 45% of all the losses of energy due to friction in the whole engine. Numerous reports suggest that the problem can be solved by applying porous surfaces generated, for example, by laser surface texturing.

The first publication on surface texturing appeared in Germany in 1995 [1]. It discussed the use of an excimer laser to texture elements of a magnetic memory disk drive with the aim of reducing friction at the

[*] Corresponding author. Tel.:48-41-34-24-539.
E-mail address: ktrba@tu.kielce.pl.

1877-7058 © 2012 Published by Elsevier Ltd. Open access under CC BY-NC-ND license.
doi:10.1016/j.proeng.2012.07.007

start. Further experiments in this area involved texturing surfaces of punches applied to plastic forming. It was found that the process caused a 169% increase in the punch service life.

The current studies focus on the influence of texturing on the performance of various friction systems in internal combustion engines, e.g. precision bearing systems. Texturing is used to improve heat removal, vaporization, wettability, biological functions, absorptivity, etc.

Reference [5] analyzes the relationships between the parameters of performance and the parameters of surface texture for a mechanical seal. In this model approach, the considerations involve solving the Reynolds equation transformed into a dimensionless form for a face seal with one textured ring. The texture is created by a number of circular pores. The radius of a pore is several times greater than the depth. The results of the theoretical investigations are presented in the form of dimensionless relations, including the ratio of the cavity depth to the cavity diameter and the ratio of the area with pores to the whole surface area (pore area coverage) as well as the dimensionless pressure and the leak tightness, Λ.

$$\Lambda = \frac{6 \cdot \mu \cdot U \cdot r_p}{p_a \cdot C^2},$$

where: μ - fluid dynamic viscosity, [Pa s]; U – sliding velocity, [m/s]; P_a – ambient pressure, [Pa]; C –clearance height, [m]; r_p – cavity diameter, [m].

The references quoted in this paper indicate that the cavity diameter and the pore area coverage have a negligible effect on the average pressure in the clearance. Of importance, however, seems to be the depth-to-diameter ratio, which can be optimized for the pre-determined parameter Λ. From the analysis it is clear that the effectiveness of micropores is dependent on the relationships between the hydrostatic and hydrodynamic effects. If the cavitation in micropores is eliminated by applying suitable parameters of performance, then the hydrostatic effects predominate and the effect of laser texturing is not significant; in consequence**,** the surfaces behave like non-textured ones.

An increase in the parameter Λ causes that the hydrodynamic effect of microcavities is more visible. The effect is determined basing on the value of the average pressure in the clearance. In addition, there exists an optimal value of $h_p/2r_p$, which is equal to 0.05 for Λ=1, and decreases with an increase in the parameter Λ.

Reference [3] compares results of tribological tests conducted by means of pin-on-disk devices, where the disk surfaces were polished, ground and textured (using three methods of texturing). The textured surface was covered with laser-generated pores, 4-6.5 μm in depth and 58-80 μm in diameter. Numerous tests show that texturing can be used to extend the ranges of load and sliding velocity within which hydrodynamic lubrication occurs. The hydrodynamic lubrication is observed when low- and high-viscosity lubricants are applied. Another finding is that the rough rims of cavities produced by laser beams need to be removed by lapping to ensure an optimal hydrodynamic effect. A comparative analysis was conducted to determine the friction coefficients for the polished, ground and textured surfaces. The effects of laser texturing were most visible when the values of sliding velocity were low, ranging between 0.075 and 0.3 m/s. Moreover, the high density of cavities was responsible for an increase in the friction coefficient. The results presented in the form of Stribeck curves illustrate that there was a significant reduction in friction for lubricated friction pairs operating in the boundary regime of friction.

The tests described in Ref. [4] aimed at determining the effect of laser texturing on the performance of a ring being in contact with a cylinder liner. Pores with diameters of 75-78 μm and depths of 7-9 μm covered the whole or parts of the ring surface. The pore area coverage ranged between 10 and 50%. The friction observed for textured surfaces was lower than that for non-textured ones. The greatest falls in friction were reported for a pore area coverage of 30%; they were 40-45% and 23-35% for a rotational speed of 500 rev/min and 1200 rev/min, respectively. It should be noted that the decrease in friction was

greater for a partly textured ring. This reduction (12–29%) was observed in the whole range of loads and rotational speeds.

Reference [6] discusses results of in-service tests conducted for face seals with textured carbide rings used in the petrochemical industry. The results were positive, because there was a decrease in the process temperature and an increase in the ring service life. Reference [7] illustrates that laser surface texturing caused an improvement in fretting fatigue life of steel tool elements.

1. Model fluid flow in the clearance between one smooth and one textured surface

Effective numerical modelling of fluid flows in clearances of sliding pairs requires considering only the basic parameters of flow and neglecting the less important ones. The parameters that are crucial to this phenomenon can be selected on the basis of a dimensional analysis and general knowledge of physics. Considering all the parameters would mean having to solve full Navier-Stokes equations, which is impossible at the present state of knowledge and computer technology, even though the Reynolds number is very small. In the case of sliding pairs, we may need to consider a two-phase flow in areas where cavitation of the oil film occurs. Since it is generally known that all the hydrodynamic effects of interest, including the hydrodynamic force formation, are related to cavitation, the phenomenon cannot be omitted. The modelling, however, will have an approximate character, which is a significant problem in any simulation. The literature shows that different physical effects have been taken into account.

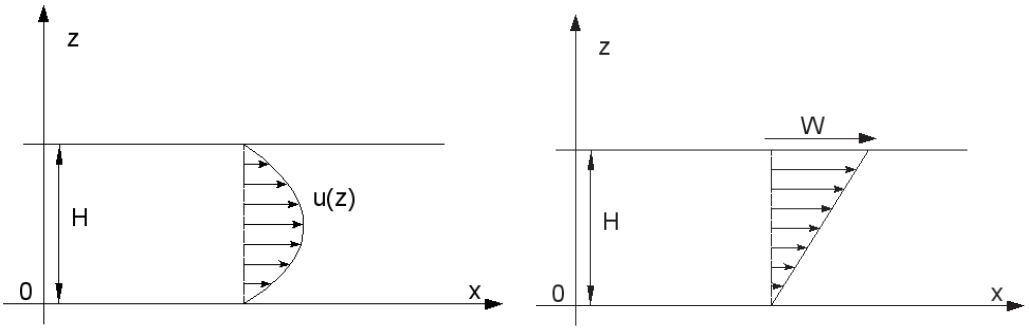

Fig. 1. Basic flows in the clearance (a) Poiseuille flow, (b) Couette flow

If the changes in the x and y directions are much slower than those in the z direction (condition H<<L), one can assume that $\vec{Q}$ is a superposition of the basic Poiseuille and Couette flows.

Thus, the equation derived for the oil film is:

$$div(\frac{\rho H^3}{6\eta} grad(p)) = div(\rho H \vec{W}),$$

where: ρ, η, H, p can be slowly-changing functions of x and y.
After integrating the equation in any domain Ω (in the x,y plane), we obtain:

$$\int_\Omega div(\frac{\rho H^3}{6\eta} grad(p))d\Omega = \int_\Omega div(\rho H \vec{W})d\Omega.$$

Then, applying the Green formula, we have:

$$\int_{\partial\Omega} \frac{\rho H^3}{6\eta} \frac{\partial p}{\partial n} d\sigma = \int_{\partial\Omega} \rho H \bar{W} \vec{n}\, d\sigma,$$

(∂Ω - the boundary of the domain Ω, and $\vec{n}$ - external normal to that boundary).

Let the domain Ω be an unit cell of a network covering the area of flow. The modelling will be performed using the example of a thrust bearing or a face seal as a friction pair.

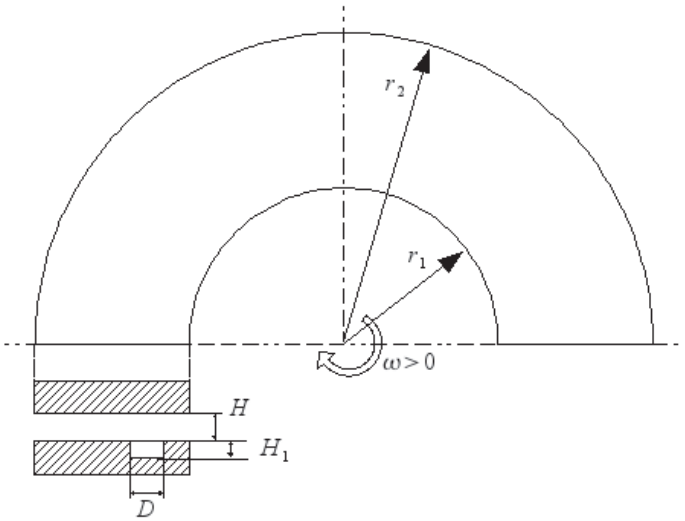

Fig. 2. Schematic diagram of the model clearance

If the coordinate system is related to the symmetry axis of the friction system, then:

$$\vec{W} = \omega r \hat{i}_0,$$

where ω is the rotational speed, r is the radius vector, and $\hat{i}_0$ is the circumferential unit vector perpendicular to r.

In the above formulae, the clearance height *H* is a variable function of position used for describing the geometry of pores produced on the bearing races by laser surface texturing.

The equation for the oil film in the fluid flow area is solved to determine the pressure area, p(x,y). The other elements are assumed to be known. The condition for pressure on the boundary of the domain is obvious, because the values of pressure around the inner and outer circumferences of the sliding ring are known.

It is assumed that the pressure in the cavitation area (where pressure falls below the boiling pressure p_{boil}) is constant, and the pressure gradient is equal to zero. In this domain, the equation of the oil film is still valid. On the left-hand side, all the terms disappear, while the right-hand side terms are used to calculate the unknown density area ρ(x,y), and, accordingly, the amount of the fluid evaporated.

On the boundary of the cavitation domain, the following conditions are satisfied:

inlet: the pressure inside is continuous, $\frac{\partial p}{\partial n} = 0$; the fluid fluxes inside and outside are identical;
outlet: the density around the outer circumference is equal to the fluid density; the fluid fluxes around the inner and outer circumferences are equal.

The integral quantities of practical interest are:

The hydrodynamic force, which can be calculated from the formula:

$$F = \int_{r_1}^{r_2}\int_{0}^{2\pi} r(p - p_{atm})d\Theta dr,$$

where: r_1 and r_2 - inner and outer radii of the ring, and p_{atm} - atmospheric pressure.

The leakage can be determined for any radius *r* using the following formula:

$$Q = \int_{0}^{2\pi} \frac{r\rho H^3}{12\eta}\frac{\partial p}{\partial r}d\Theta,$$

it is desirable, however, to average the number by integration applying different radius to increase the accuracy of calculation:

$$Q = \frac{1}{r_2 - r_1}\int_{0}^{r}\int_{0}^{2\pi} \frac{r\rho H^3}{12\eta}\frac{\partial p}{\partial r}d\Theta dr.$$

The torque representing the frictional resistance is determined as an integral of tangential stresses by means of the formula:

$$M = \omega\int_{r_1}^{r_2}\int_{0}^{2\pi} \frac{r\eta}{H}d\Theta dr - \frac{1}{2}\int_{r_1}^{r_2}\int_{0}^{2\pi} rH\frac{\partial p}{\partial \Theta}d\Theta dr.$$

In numerical calculations, the hydrodynamic force F generated by a single element of the texture was replaced by:

$$P_{av} = \frac{F}{\pi D^2/4},$$

where: the denominator corresponds to the pore surface area. Accordingly, the quantity P_{av} [Pa] corresponds to the average pressure acting on the etched part of the race. The total force acting on the seal is calculated as:

$$F_{total} = P_{av} \cdot S \cdot C,$$

where: S – race area, and C – dimensionless pore area coverage (percentage of pores in a whole surface).

Figure 3 indicates the variation of P_{av} in relation to the rotational speed ω and the clearance height H. The other parameters are standard.

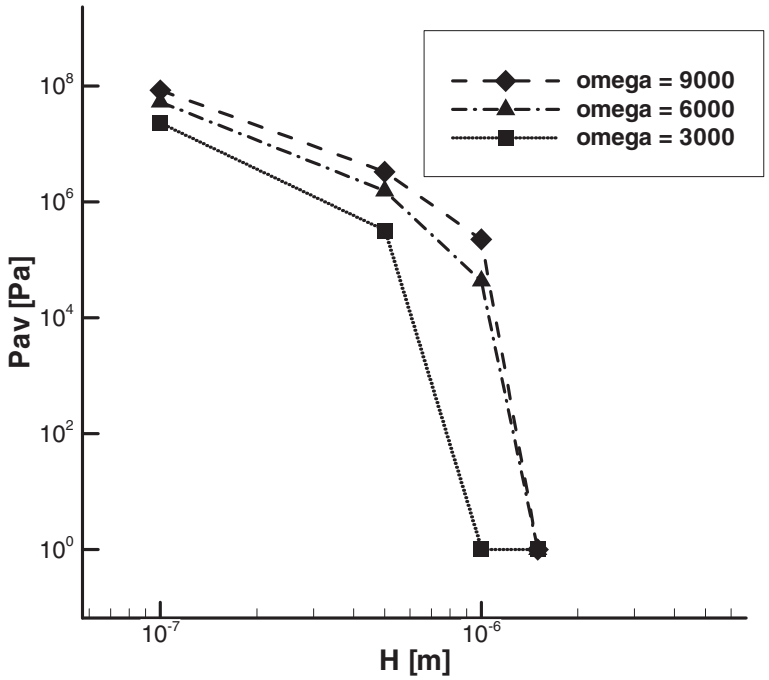

Fig. 3. Relationship between the average pressure, the clearance height and the rotational speed

Figure 4 presents the relationship between P_{av}, the pore diameter [μm] and the pore depth [m]. The other parameters are standard.

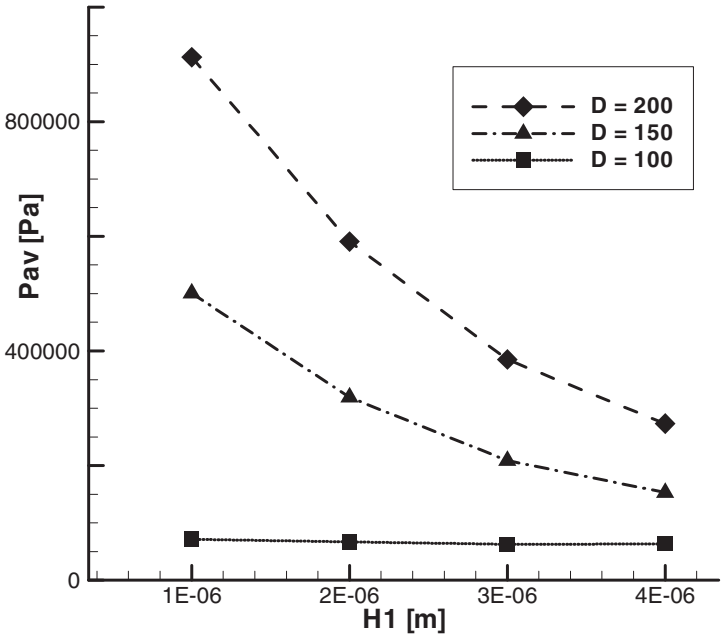

Fig. 4. Relationship between the average pressure, the pore depth and the pore diameter

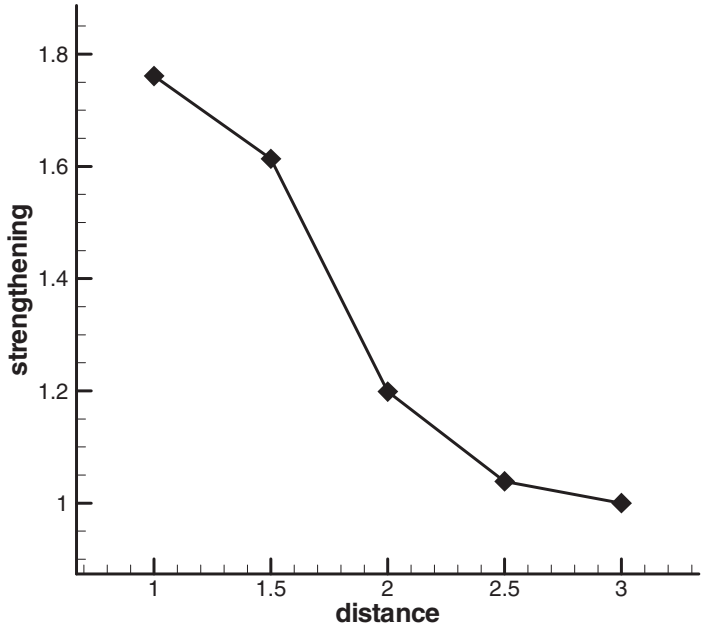

Fig. 5. Hydrodynamic force amplification versus radial distance between pores

Figure 5 illustrates the relationship between the hydrodynamic force amplification and the radial distance between the texture cavities. A multiple pore diameter is shown in the X-axis. The other parameters are standard. A decrease in the radial distance between cavities causes almost a double increase in the hydrodynamic force.

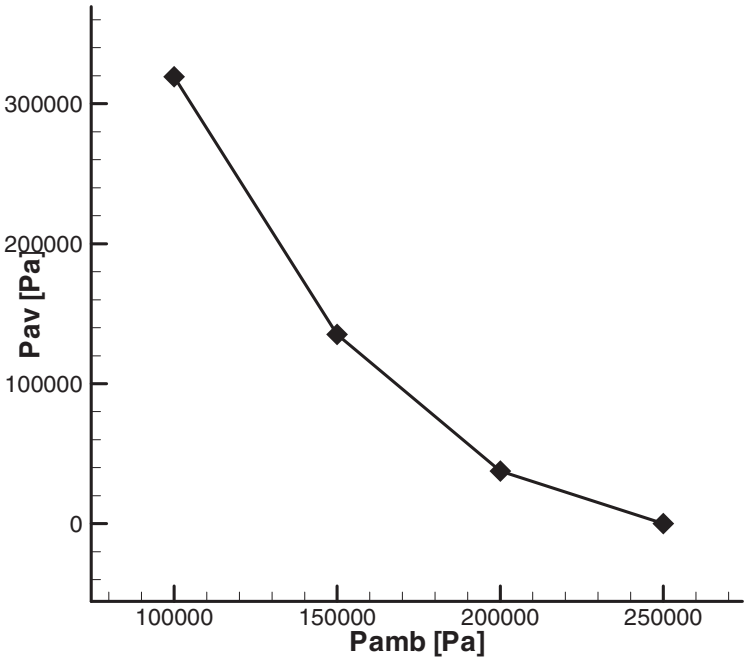

Fig. 6. Average pressure versus ambient pressure

Figure 6 shows the effect of ambient pressure on the hydrodynamic force. In the previous diagrams, the ambient pressure corresponded to the atmospheric pressure. An increase in this pressure resulted in a considerable decrease in the hydrodynamic force. Technically, the pressures around the inner and outer edges of the friction elements are different, as is the case of face seals. Pores in the area of higher pressure will generate a hydrodynamic force that is smaller than those around the outer edge.

2. Laser surface texturing

The surfaces of the rings were textured using a diode-pumped Nd:YAG laser, designed for the production of printed circuit boards. The laser emits ultraviolet light, and the wavelengths are specially selected to assure the most effective machining of copper. The maximum power of the laser beam is 2W. The laser can be applied to drill microholes in laminates, for instance, copper-clad laminates, which are used for printed circuit boards. The device can be employed also to cut or drill holes in other materials; the maximum beam power, however, limits its application. It is suitable for cutting metal foils: steel and nickel up to 100 μm in thickness, and copper up to 200 μm in thickness. The maximum hit rate for this type of laser is more than 20000 holes per hour. The focal spot size is 25 μm.

The application of a laser beam causes laser ablation of the material. The photon energy is converted on the material surface into electron, thermal and mechanical energies. In consequence, the material in contact with the laser beam is vapourized and removed from the solid surface in the form of neutral atoms and molecules, and positive and negative ions.

Device performance characteristic:

Producer: *Electro Scientific Industries*
Type of device: *Model 5200*
Type of laser: *diode-pumped Nd:YAG laser, UV [355nm]*
Peak power: *>15 kW for 3 kHz*
Pulse width: *30 nsek for 3 kHz*
Frequency: *100 Hz ÷ 20 kHz*
Field size: *533 mm x 635 mm*

Laser surface texturing is one of the most common and promising methods of surface roughening. Categorized as a metal removal process, laser texturing is usually performed at a power density of $10^6 \div 10^9$ W/cm^2. At present, it accounts for about 2 % of all laser-based material processing processes used in the world. In laser surface texturing, a pulsed laser beam is focused on a material to melt a hole. The hole depth is dependent mainly on the power density and the pulse duration. The drilling debris is removed from a hole being drilled using compressed air or another inert gas.

The tests were conducted for SiC rings (certificate of material excellence) with the following dimensions: an outer diameter d_o of 35.3 mm, an inner diameter d_i of 25.1 mm, and a height h of 7 mm. The texturing was performed using an ESI 5200 Nd:YAG laser (pulse mode). The wavelength λ= 355 nm (the laser uses radiation at the third harmonic frequency).

The parameters of the laser surface texturing process were determined basing on the experimental results: the laser spot diameter d = 0.78÷150 μm; the laser power P = 0.37÷0.4 W; the laser beam velocity V = 15.7÷23.56 mm/s; the distance from the focus Δf = 0 mm; and the repetition frequency f = 6400 Hz.

The process of texturing was performed in two stages (two steps). In the fist step, holes with a pre-determined diameter were drilled along a spiral path. In the second step, the drilling debris was removed from each pore, with the number and frequency of pulses being strictly defined.

Table 1. Parameters of the ring surface texture

Ring number	Pore diameter [μm]	Distance between the centres of adjacent pores [μm]	Pore area coverage [%]	Number of pores *k* [-]	Pore volume [mm^3]
1	78	162	18.208	18440	0.693
2	134	279	17.985	6216	0.668
3	78	106	42.520	43060	1.619
4	134	183	41.808	14450	1.553
5	150	256	27.464	7383	0.992
6	70	119	27.173	34170	1.047
7	102	128	49.951	29530	1.865
8	102	233	15.051	8913	0.562
9	102	174	26.985	15980	1.008
10	102	174	26.985	15980	1.008

(pore depth 13μm)

The main stage of the process was drilling a pore with a predetermined shape, diameter, and depth. The material processed was particularly susceptible to the action of the laser beam. Ablation occurred at low beam energy.

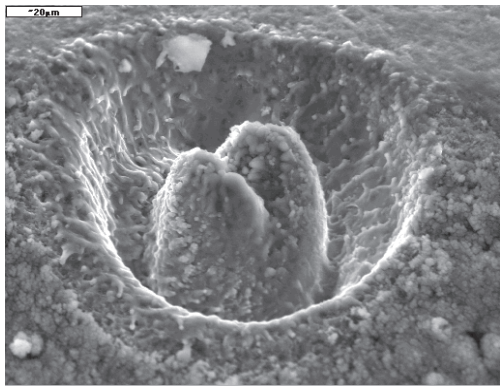

Fig. 7. A pore produced in an SiC ring in the first step of the laser operation along a spiral trajectory (magnification 1000x)

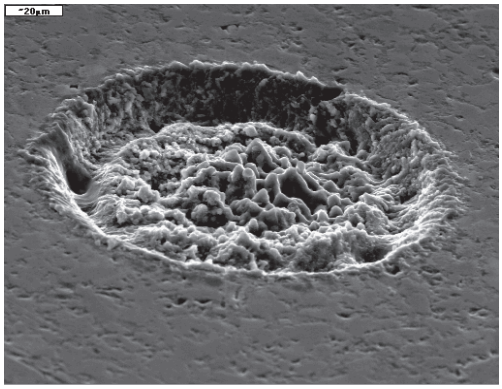

Fig. 8. A pore generated in an SiC ring in the second step of the laser operation after cleaning the pore bottom (magnification x750)

A Joel JSM-5400 scanning electron microscope was used to study the effects of laser surface texturing. Selected SEM images are presented in Figs. 7÷8 and 9÷10. As can be seen, the surface structure after laser surface texturing is regular. The surface is covered by bumps and dimples resulting from phase and structural modifications and the accompanying specific volume changes in the laser affected zones.

Lapping and superfinish are used to obtain hard flat areas transferring normal loads and areas of pores where the hydrodynamic forces are generated during fluid lubrication. Surfaces with such a texture can be applied, for instance, to sliding friction systems.

The microscopic analysis showed that the removal of the drilling debris was not complete when the laser beam was focused locally. This was probably due to insufficient power density. The action of the thermocapillary forces and the convective motion resulted in the formation of rims, whose structure consisted of molten and then crystallized SiC.

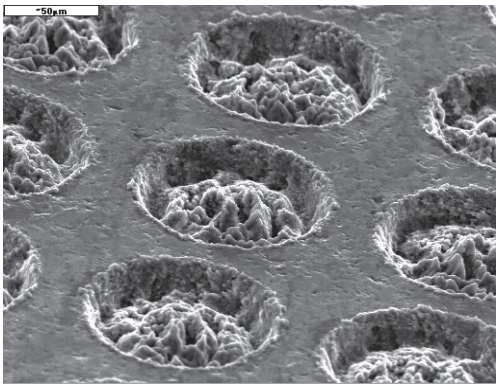

Fig. 9. A view of pores on the SiC ring (magnification x25)

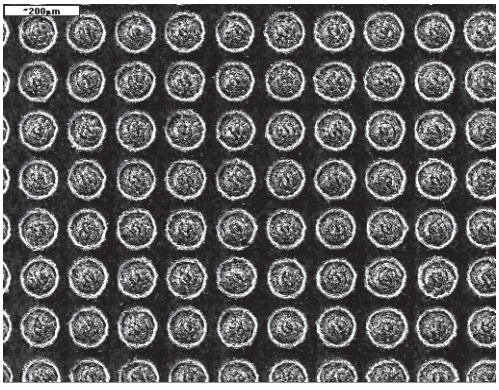

Fig. 10. A view of a system of pores on a SiC ring; pore area coverage - 42% (magnification x100)

Pores generated with the aim of improving the tribological properties of the material were arranged regularly. In this analysis, we deal with a two-directional symmetry. It can be assumed that surface modelling involves producing blind holes in the shape of a cylinder or, more frequently, a truncated cone.

3. Conclusions

Ad. Modelling of fluid flow

The following conclusions were drawn basing on the qualitative results of the simulations:

- as expected, the hydrodynamic force was greatly dependent on the rotational speed and the clearance height;
- on surfaces where pores were larger in depth and diameter, the pressure was higher and the hydrodynamic force was larger;
- the smaller the radial distance between the pores, the larger the hydrodynamic force;
- no such effect was observed in the circumferential direction;
- the greatest effect of surface texturing was reported in the low-pressure zone (around the outer circumference of the race).

Ad. Laser forming of texture

- The process of laser surface texturing performed by means of an ESI 5200 Nd:YAG laser μvia drill can be applied to produce predetermined pore patterns on sliding surfaces. Pores on metallic materials are reproducible in shape and depth; for SiC, reproducibility may reach a value of the order of several dozen μm.
- The software of the ESI 5200 Nd:YAG laser μvia drill can be used for texturing flat surfaces. Special-purpose equipment and software need to be applied to texture cylindrical and other curvilinear surfaces.
- The pore shape is limited by the software used. Standard procedures allow drilling circular holes. Specially developed programs are necessary to drill holes other than circular.

References

[1] Etsion I. *State of the Art in Laser Surface Texturing.* Transaction of the ASME January 2005, Vol. 127.

[2] X.Q Yu, S.He, R.L.Cai. *Frictional characteristics of mechanical seals with a laser textured seal face*. Journal of Materials Processing Technology 129 (2002), pp. 463-466.

[3] Kovalchenko A., Ajayi A., Erdemir A, Fenske G, Etison I. *The effect of laser surface texturing on transitions in lubrication regimes during unidirectional sliding contact*. Tribology International 38 (2005), pp. 219-225.

[4] Etsion I. *A laser surface textured hydrostatic mechanical seal.* Sealing technology March 2003.

[5] Erdemir A. *Review of engineered tribological interfaces for improved boundary lubrication.* Tribology International 38 (2005), pp. 249-256.

[6] Mcgeough J.A., Rasmussen H. *A theoretical model of electrodischarge texturing*. Journal of Materials Processing Technology 68 (1997), pp. 172-178.

[7] Volchok A., Halperin G, Etsion I. *The effect of surface regular microtopography on fretting fatigue life*. Wear 235 (2002), pp. 509-515.

[8] Wakuda M., Yamauchi Y., Kanazaki S., Yasuda Y. *Effect of surface texturing on friction reduction between ceramic and steel materials under lubricated sliding contact*. Wear 254 (2003), pp. 356-363.

[9] Antoszewski B., Rokicki J. *Tribology aspect of the laser treatment for mechanical seals.* 15th Inter. Conf. on Fluid Sealing, Maastricht, BHR Group Conference Series Publication No.26 (1997), pp. 27-37.

[10] Antoszewski B. *Własności laserowo i plazmowo modyfikowanych ślizgowych węzłów tarcia na przykładzie uszczelnień czołowych.* Monografia nr 17 (1999), Kielce.

[11] Lionel A., Young B., Key R., Philips R., Svendsten S. *Mechanical seals with laser machined wavy SiC faces for high duty boiler circulation and feedwater applications.* Lubrication Engineering. Vol. 59, Iss. 4 (April 2003), p. 30, 10 p.